

# In-gap state and effect of light illumination in $\text{CuIr}_2\text{S}_4$ probed by photoemission spectroscopy

K. Takubo,<sup>1</sup> T. Mizokawa,<sup>1</sup> N. Matsumoto,<sup>2</sup> and S. Nagata<sup>2</sup>

<sup>1</sup>*Department of Physics and Department of Complexity Science and Engineering, University of Tokyo, 5-1-5 Kashiwanoha, Chiba 277-8581, Japan*

<sup>2</sup>*Department of Materials Science and Engineering, Muroran Institute of Technology, 27-1 Mizumoto-cho, Muroran, Hokkaido 050-8585, Japan*

(Received 13 August 2008; revised manuscript received 29 October 2008; published 19 December 2008)

We have studied disorder-induced in-gap states and effect of light illumination in the insulating phase of spinel-type  $\text{CuIr}_2\text{S}_4$  using ultraviolet photoemission spectroscopy (UPS). The  $\text{Ir}^{3+}/\text{Ir}^{4+}$  charge-ordered gap appears below the metal-insulator transition temperature. However, in the insulating phase, in-gap spectral features with *softgap* are observed in UPS just below the Fermi level ( $E_F$ ), corresponding to the variable range hopping transport observed in resistivity. The spectral weight at  $E_F$  is not increased by light illumination, indicating that the  $\text{Ir}^{4+}$ - $\text{Ir}^{4+}$  dimer is very robust, although the long-range octamer order would be destructed by the photoexcitation. Present results suggest that the  $\text{Ir}^{4+}$ - $\text{Ir}^{4+}$  bipolaronic hopping and disorder effects are responsible for the conductivity of  $\text{CuIr}_2\text{S}_4$ .

DOI: 10.1103/PhysRevB.78.245117

PACS number(s): 71.30.+h, 79.60.-i

## I. INTRODUCTION

When some disorders are introduced in Mott insulators or charge-ordered insulators, disorder-induced electronic states are often observed within the band gaps and are responsible for the hopping transport in the insulating phase.<sup>1-4</sup> Although it is very important to understand the relationship between the transport behaviors and the disorder-induced in-gap states, no unified picture on the relationship is obtained so far. For example, in  $\text{Ca}_{2-x}\text{Sr}_x\text{RuO}_4$ ,<sup>1</sup>  $\text{NiS}_{2-x}\text{Se}_x$ ,<sup>2</sup> and  $\text{R}_{1-x}\text{A}_x\text{MnO}_3$ ,<sup>3</sup> almost localized electronic states are formed within the band gap and are responsible for the variable range hopping (VRH) transport. On the other hand, in lightly doped  $\text{La}_{2-x}\text{Sr}_x\text{CuO}_4$  ( $x=0.03$ ), a sharp peak with clear band dispersion is observed within the Mott gap while the resistivity shows a VRH behavior.<sup>4</sup> The VRH transports and in-gap states suggest that the insulating and metallic clusters coexist near the metal-insulator transition (MIT) in these materials.<sup>5,6</sup> Such inhomogeneity plays crucial roles in their remarkable properties of colossal magnetoresistance and photoinduced MIT in manganites<sup>7,8</sup> and stripe formation in cuprates.<sup>9</sup>

$\text{CuIr}_2\text{S}_4$  with spinel structure is one of such systems and shows a MIT at  $T_{\text{MI}} \sim 226$  K.<sup>10-16</sup> The anomalous hopping transport is also observed in the insulating phase  $\rho \propto \exp[-(T/T_0)^{1/2}]$  (Refs. 17 and 18) or  $\rho \propto A \exp(-E_a/k_B T) + B \exp[-(T/T_0)^{1/4}]$ .<sup>19,20</sup> The temperature variation in  $\rho \propto \exp[-(T/T_0)^{1/2}]$  can be described by a Mott VRH conductivity in one-dimensional case<sup>21</sup> or by an Efros-Shklovskii VRH conductivity.<sup>22</sup> However, a rather complicated three-dimensional charge ordering of  $\text{Ir}^{3+}$  ( $S=0$ ) and  $\text{Ir}^{4+}$  ( $S=1/2$ ) sites is indicated in the insulating phase of  $\text{CuIr}_2\text{S}_4$ .<sup>23</sup> The cubic spinel structure of  $\text{CuIr}_2\text{S}_4$  becomes tetragonally elongated along the  $c$  axis, and biccapped hexagonal ring octamers of  $\text{Ir}^{3+}$  and  $\text{Ir}^{4+}$  are formed below  $T_{\text{MI}}$ . The orbital-driven Peierls mechanism has been suggested<sup>24</sup> in which the  $\text{Ir}^{4+}$  ions are dimerized along  $xy$  chains of the  $B$  sites. Moreover, the resistivity of  $\text{CuIr}_2\text{S}_4$  is reduced by x-ray,<sup>25,26</sup> visible-light,<sup>27,28</sup> or electron-beam irradiation<sup>29,30</sup> at low temperature ( $\sim 100$  K). The symmetry of crystal is changed from triclinic to tetragonal by the irradiation, and the photo-

induced state has a long lifetime. It has been proposed that the photoexcitation breaks the  $\text{Ir}^{3+}/\text{Ir}^{4+}$  charge ordering and induces the metallic conductivity.

The indication of MIT and the  $\text{Ir}^{3+}/\text{Ir}^{4+}$  charge ordering have been obtained on previous x-ray photoemission and absorption studies of  $\text{CuIr}_2\text{S}_4$ .<sup>27,31-35</sup> The Ir  $4f$  core-level spectrum of the insulating phase has two components with large energy difference, consistent with the charge ordering of Ir sites.<sup>27,35</sup> In contrast, the core-level spectrum has not been changed against laser irradiation, while the resistivity is reduced.

In this paper, we report results of ultraviolet photoemission spectroscopy (UPS) of  $\text{CuIr}_2\text{S}_4$  single crystals combined with laser illumination. The UPS spectrum shows a clear MIT with band-gap opening of  $\sim 0.09$  eV. However, the UPS spectrum just below the Fermi level ( $E_F$ ) at low temperature ( $\sim 20$  K) has a peculiar power-law dependence of  $\sim (E-E_F)^n$ , where  $n \sim 1.3-1.7$ , that is associated with the anomalous conduction. The systematic spectral change in UPS against laser irradiation has not been observed. The  $\text{Ir}^{4+}$ - $\text{Ir}^{4+}$  dimers in the  $xy$  plane of spinel are very robust against photoexcitation and play important roles in exotic conduction.

## II. EXPERIMENTS

Single crystals of  $\text{CuIr}_2\text{S}_4$  were grown by the bismuth solution method, described previously in detail.<sup>36</sup> UPS measurements were performed using Scienta SES-100 spectrometers equipped with a He I source ( $h\nu=21.2$  eV). The total resolution was 30 meV, and the base pressure of the spectrometer was  $1 \times 10^{-7}$  Pa. Five  $\text{CuIr}_2\text{S}_4$  single crystals were studied for UPS measurements. The first and second samples named R1 and R2 are cleaved at 300 K *in situ* and then measured at various temperatures. The third, fourth, and fifth samples named L3, L4, and L5 are cleaved at 20 K *in situ* and then measured at various temperatures. All photoemission data were collected within 24 h after the cleaving. In order to study the effects of visible-light excitation, a Nd:YAG (yttrium aluminum garnet) pulsed laser provided

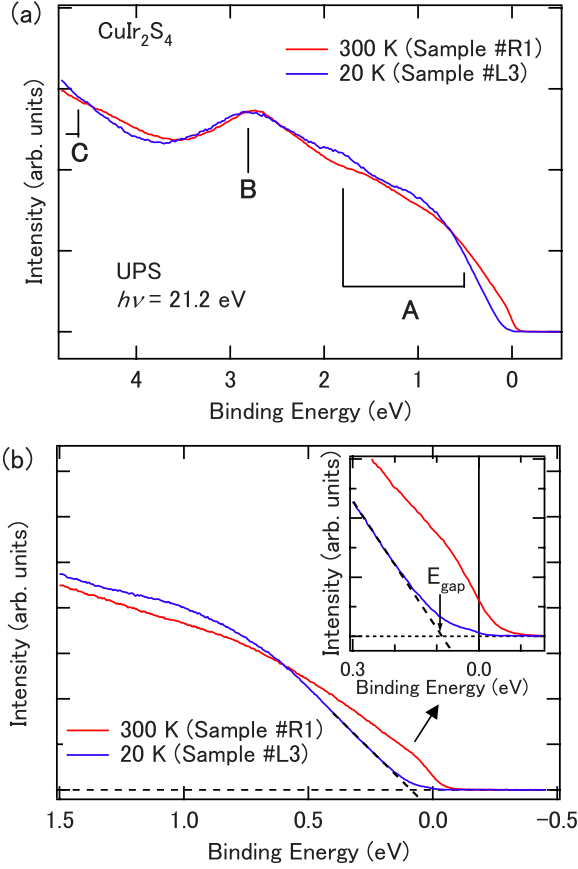


FIG. 1. (Color online) UPS of  $\text{CuIr}_2\text{S}_4$  taken at 300 and 20 K immediately after cleaving. (a) Wide-range spectra. (b) Near- $E_F$  spectra. Inset of (b) shows the expanded spectra near  $E_F$ .

optical excitation to the samples at energies of 2.3 eV (532 nm) with a pulse frequency of 30 Hz and a pulse width of about 10 ns. The beam was focused to a spot of 4 mm diameter.

### III. RESULTS AND DISCUSSIONS

#### A. Temperature dependence

Figure 1 shows wide-range UPS of  $\text{CuIr}_2\text{S}_4$  taken at 300 K for sample R1 and 20 K for sample L3 immediately after cleaving, respectively. Compared with the previous studies,<sup>27,31,32,37,38</sup> structures A, B, and C are assigned to the Ir  $5d$ -S  $3p$  antibonding band, the Cu  $3d$  band, and the Ir  $5d$ -S  $3p$  bonding band, respectively. In the near- $E_F$  spectra, a spectral change across the MIT is observed. The intensity at  $E_F$  is substantial in the spectrum at 300 K (sample R1; red line; metallic phase), while the intensity at  $E_F$  almost disappears in the spectrum at 20 K (sample L3; blue line; insulating phase) [see Fig. 1(b)]. The opening of the gap  $E_{\text{gap}} \sim 0.09$  eV, obtained by extrapolating the slope near the valence-band maximum to the base line, agrees with the previous photoemission results<sup>16,27,35</sup> and is attributed to the Ir<sup>3+</sup>/Ir<sup>4+</sup> charge ordering and Ir<sup>4+</sup>-Ir<sup>4+</sup> dimerization along the  $xy$  chains with the tetragonal distortion.

The spectrum of the insulating phase has a tail above the valence-band maximum that reaches  $E_F$  and forms a kind of

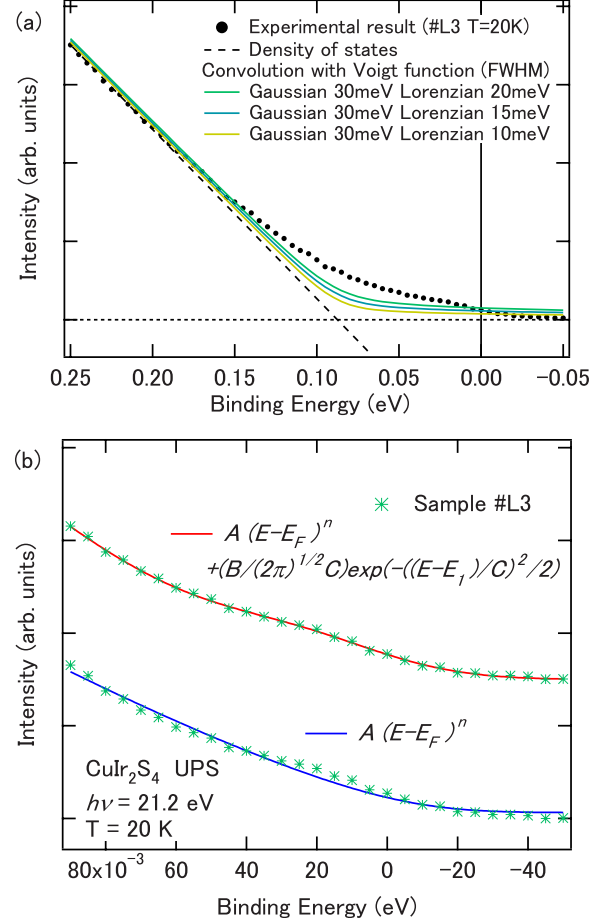


FIG. 2. (Color online) (a) Density of states near the valence-band maximum convoluted with the Voigt function with Gaussian FWHM of 30 meV and various Lorentzian FWHMs (10, 15, and 20 meV). UPS of  $\text{CuIr}_2\text{S}_4$  at 20 K (L3) is indicated by the black dotted curve. (b) In-gap region of UPS for sample L3 taken at 20 K immediately after cleaving. The solid curves indicate the fitted results with model functions  $A(E-E_F)^n + \frac{B}{\sqrt{2\pi}C} \exp[-(\frac{E-E_1}{C})^2/2]$  and  $A(E-E_0)^n$ .

TABLE I. Best-fit parameters of the model functions  $A(E-E_F)^n + \frac{B}{\sqrt{2\pi}C} \exp[-(\frac{E-E_1}{C})^2/2]$  and  $A(E-E_0)^n$  for the spectra of sample L3 of  $\text{CuIr}_2\text{S}_4$ . The spectra are normalized using integrated intensity of up to 0.09 eV.

Function: $A(E-E_F)^n + \frac{B}{\sqrt{2\pi}C} \exp[-(\frac{E-E_1}{C})^2/2]$				
Sample (20 K)	$n$	$B$	$C$ (eV)	$E_1$ (eV)
L3	$1.5 \pm 0.2$	$0.23 \pm 0.03$	$0.02 \pm 0.01$	$0.02 \pm 0.01$
Function: $A(E-E_0)^n$				
Sample (20 K)	$n$	$B$	$C$ (eV)	$E_1$ (eV)
L3	$1.7 \pm 0.2$			

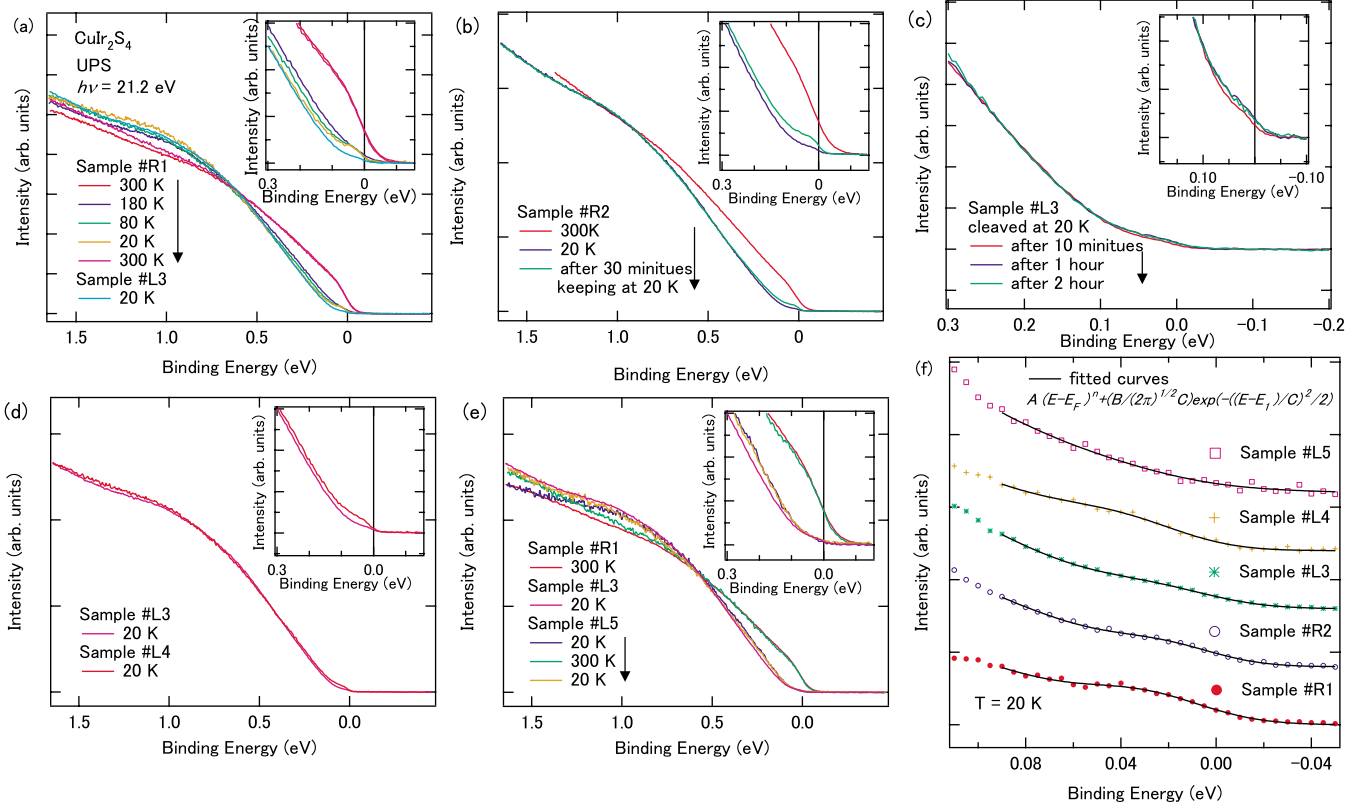


FIG. 3. (Color online) UPS data of  $\text{CuIr}_2\text{S}_4$  taken at various temperatures and for various samples. [(a)–(e)] Insets are the expanded spectra near  $E_F$ . The arrows denote the order of the measurements. (f) Near- $E_F$  region of UPS data for  $\text{CuIr}_2\text{S}_4$  taken at 20 K. The solid curves indicate the fitted results with model functions  $A(E-E_F)^n + \frac{B}{\sqrt{2\pi}C} \exp[-(\frac{E-E_1}{\sqrt{2}C})^2]$ .

softgap, interestingly. In order to confirm the existence of the in-gap state at the insulating phase, the density of states near the valence-band maximum [indicated by the dashed curve in Fig. 1(b)] is convoluted with the Voigt function with Gaussian full width at half maximum (FWHM) of 30 meV and various Lorentzian FWHMs (10, 15, and 20 meV). As shown in Fig. 2(a), the intensity of the observed tail part is much stronger than that expected from the broadening of the valence band with the Voigt functions. This observation directly corresponds to the anomalous hopping transport observed in the resistivity measurements  $\rho \propto \exp[-(T/T_0)^{1/2}]$

TABLE II. Best-fit parameters of the model function  $A(E-E_F)^n + \frac{B}{\sqrt{2\pi}C} \exp[-(\frac{E-E_1}{\sqrt{2}C})^2]$  for the spectra of samples R1, R2, L3, L4, and L5 of  $\text{CuIr}_2\text{S}_4$ . The spectra are normalized using integrated intensity of up to 0.09 eV.

Function: $A(E-E_F)^n + \frac{B}{\sqrt{2\pi}C} \exp[-(\frac{E-E_1}{\sqrt{2}C})^2]$				
Sample (20 K)	$n$	$B$	$C$ (eV)	$E_1$ (eV)
R1	$1.4 \pm 0.2$	$0.38 \pm 0.03$	$0.03 \pm 0.01$	$0.03 \pm 0.01$
R2	$1.3 \pm 0.1$	$0.22 \pm 0.03$	$0.02 \pm 0.01$	$0.02 \pm 0.01$
L3	$1.5 \pm 0.2$	$0.23 \pm 0.03$	$0.02 \pm 0.01$	$0.02 \pm 0.01$
L4	$1.4 \pm 0.1$	$0.30 \pm 0.03$	$0.03 \pm 0.01$	$0.04 \pm 0.01$
L5	$1.6 \pm 0.2$	$0.24 \pm 0.03$	$0.04 \pm 0.01$	$0.03 \pm 0.01$

(Refs. 17 and 18) or  $\rho \propto A \exp(-E_a/k_B T) + B \exp[-(T/T_0)^{1/4}]$ .<sup>19,20</sup> The energy resolution is not enough to determine the line shape of the in-gap state. Here, considering the transport behavior, we assumed that the in-gap state has the shape of  $(E-E_F)^n$ . Therefore, we tried to fit this in-gap spectral feature up to 0.09 eV ( $\sim E_{\text{gap}}$ ) to two types of model functions  $A(E-E_F)^n + \frac{B}{\sqrt{2\pi}C} \exp[-(\frac{E-E_1}{\sqrt{2}C})^2]$  and  $A(E-E_0)^n$  [Fig. 2(b)]. The power-law function  $A(E-E_F)^n$  is additionally convoluted with a Gaussian function taking into account the instrumental and thermal broadenings ( $\sim 40$  meV). In addition to the intrinsic in-gap state, the hump structure is observed near the Fermi level. We have analyzed the various

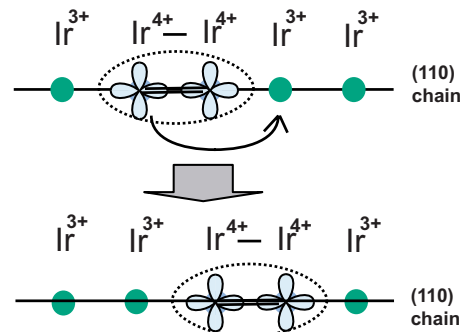


FIG. 4. (Color online) Hopping of holes between an  $\text{Ir}^{4+}\text{-Ir}^{4+}$  dimer and a neighboring  $\text{Ir}^{3+}$  site along the (110) or (-110) chains. The dimer moves without reducing the number of  $\text{Ir}^{4+}\text{-Ir}^{4+}$  bonds.

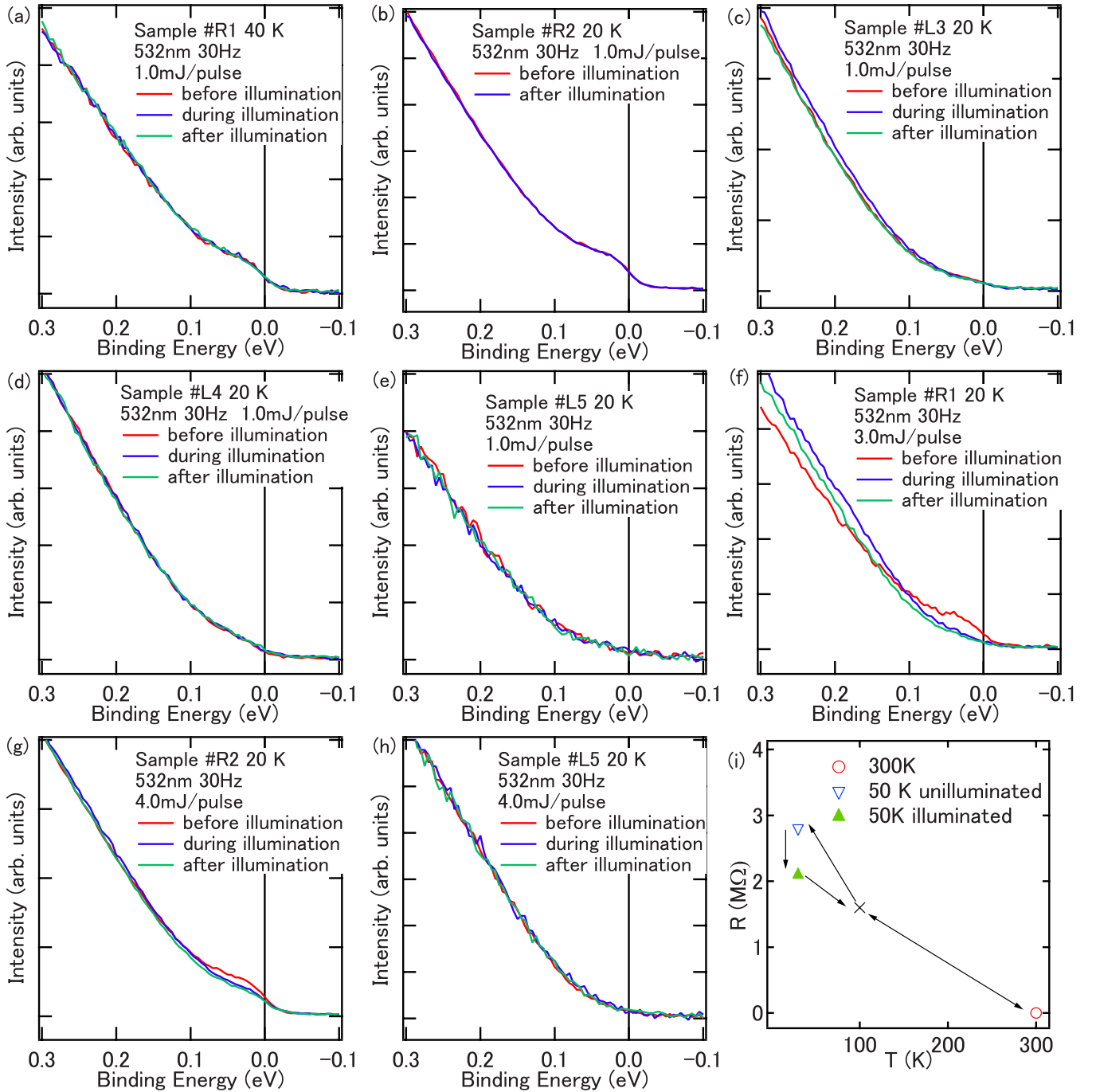


FIG. 5. (Color online) [(a)–(h)] UPS of  $\text{CuIr}_2\text{S}_4$  before, during, and after visible-light irradiation from the Nd:YAG laser (532 nm) for various samples. (i) The resistance taken under the same condition as the photoemission measurements.

spectra with various hump structure strengths (modeled by the Gaussian peak) and confirmed that the tail structure of  $(E-E_F)^n$  is common for all the spectra as shown in the next paragraph. The integrated intensity is normalized to unity, and the fitted parameters are shown in Table I. The exponent of  $n$  for sample L3 is estimated to be  $\sim 1.5$  and  $\sim 1.7$  by using the functions of  $A(E-E_F)^n + \frac{B}{\sqrt{2\pi}C} \exp[-(\frac{E-E_1}{\sqrt{2}C})^2]$  and  $A(E-E_0)^n$ , respectively.

Temperature dependence of the wide-range UPS was carefully examined for various fractured surfaces. Figure 3(a) shows temperature dependence of UPS for sample R1,

which was cleaved at 300 K and then measured with decreasing temperature. Although the spectra show the band-gap opening, a hump structure near  $E_F$  remains even at the lowest temperature  $\sim 20$  K in contrast to the spectra for sample L3 measured immediately after cleaving at 20 K. Sample R2 was also cleaved at 300 K and then measured with decreasing temperature. However on the spectrum immediately taken after cooling down, such hump is almost absent [Fig. 3(b), blue line]. Moreover after keeping 20 K for 30 min, the intense hump (green line) appeared also for sample R2. Even for sample L3, cleaved at low temperature, the intensity

gradually increased with time although the intensity is rather small compared to the samples (R1 and R2) cleaved at 300 K. Even at 20 K, the intensity of the hump depends on the cleavage. While, for sample L4 cleaved at 20 K, the hump was clearly observed; its intensity was very small for sample L5. While the hump appeared after keeping the sample at 20 K in sample R2, it did not appear after 30 min in sample L5. Probably, the hump is enhanced by some adsorbates on the surface, but the rate of adsorption strongly depends on some subtle surface condition that can be different for different cleavage. Probably, the adsorption is enhanced due to the surface state composed from unpaired  $\text{Ir}^{4+}$  at the surface. Thus the hump structure can be affected by various surface conditions including treatments such as cleaving, change in temperature, or irradiation from He I source.

We have tried to fit all the spectra taken at 20 K with the function  $A(E-E_F)^n + \frac{B}{\sqrt{2\pi}C} \exp[-(\frac{E-E_1}{\sqrt{2}C})^2]$  as shown in Fig. 3(f) and Table II. The exponents of  $n$  are universally estimated to be  $\sim 1.3-1.6$  by using this function at low temperature of  $\text{CuIr}_2\text{S}_4$ , independent of the Gaussian contribution, namely, the surface contribution. Therefore, we can safely conclude that, while the hump near  $E_F$  is the surface contributions, the in-gap state with the power-law function  $A(E-E_F)^n$  with  $n \sim 1.3-1.6$  is derived from the bulk and is responsible for the VRH transport,  $\rho \propto \exp[-(T/T_0)^{1/2}]$  (or  $\propto A' \exp(-E_a/k_B T) + B' \exp[-(T/T_0)^{1/4}]$ ).

In the situation forming softgap due to electron-electron Coulomb repulsion of Efros-Shklovskii type, the spectral function is usually characterized by  $A(E-E_F)^2$  dependence.<sup>22,39</sup> However  $\text{CuIr}_2\text{S}_4$  has complicated three-dimensional charge order and has *hardgap* of  $\sim 0.09$  eV. Probably, some disorder in the charge-ordered state is the origin of the in-gap spectral feature and the VRH transport. Recently based on transport measurements of  $\text{Ca}_{2-x}\text{Sr}_x\text{RuO}_4$ , Nakatsuji *et al.*<sup>1</sup> proposed that the hopping exponent of  $\alpha \sim 1/2$  is a universal feature of the disordered Mott system close to the metal-insulator transition and reflects the emergence of disorder-induced localized electronic states in the Mott-Hubbard gap. The presence of some kind of disorder such as coexisting metallic clusters in the insulating phase, which can be created near the first-order MIT, gives a strongly localized state and  $\alpha \sim 1/2$ . A distinct in-gap state is also observed in UPS of  $\text{Ca}_{2-x}\text{Sr}_x\text{RuO}_4$ .<sup>40</sup>

The suppressed  $n \sim 1.5$  of  $A(E-E_F)^n$  is observed in a recent photoemission study on  $\text{BaIrO}_3$ , which has a quasi-one-dimensional structure with  $\text{Ir}_3\text{O}_{12}$  trimers and also shows a charge-density wave transition.<sup>41</sup> The exponent of  $n=1.5$  for  $\text{BaIrO}_3$  is attributed to the strong influence of electron-magnon interaction. The traveling dimer conduction in low-temperature phase of  $\text{CuIr}_2\text{S}_4$  is proposed in Ref. 18. All  $\text{Ir}^{4+}$  holes at low-temperature fall in the  $xy$  orbitals and form the dimers along the (110) [or (-110)] chains.<sup>24</sup> When the  $\text{Ir}^{4+}-\text{Ir}^{4+}$  dimer bonds are very strong and the system has good one dimensionality, single hole hopping from an  $\text{Ir}^{4+}-\text{Ir}^{4+}$  dimer to a neighboring  $\text{Ir}^{3+}$  site along the (110) chain may be suppressed. Instead, paired hole hopping (bipolaronic hopping) of an  $\text{Ir}^{4+}-\text{Ir}^{4+}$  pair along the (110) chain is favored as shown in Fig. 4. The paired hole conduction may have quasi-one-dimensional and bipolaronic features in

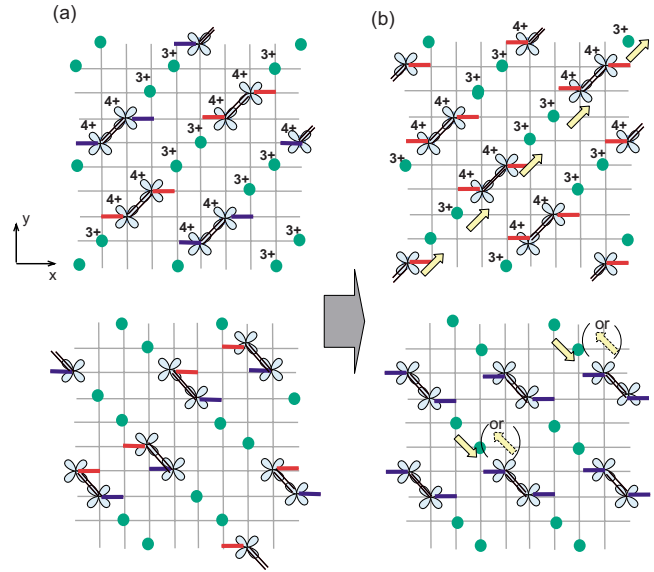


FIG. 6. (Color online) (a) Charge ordering of Ir sites of  $\text{CuIr}_2\text{S}_4$  sitting in one  $xy$  plane. The lower panel is another  $xy$  plane  $a/4$  below upper panel. The double solid lines denote the  $\text{Ir}^{4+}-\text{Ir}^{4+}$  dimerized bonds. The bold lines toward  $x$  direction denote the octamer bonding toward  $\text{Ir}^{4+}$  in the different planes. (b) When the  $\text{Ir}^{4+}-\text{Ir}^{4+}$  dimers shift by one unit, the octamer ordering is destroyed and another order may appear.

the (110) or (-110) chains even in the three-dimensional lattice. Actually, the UPS line shapes of  $\text{CuIr}_2\text{S}_4$  across the MIT resemble those of a bipolaronic material  $\text{Ti}_4\text{O}_7$ .<sup>42</sup> The spectral weight in the insulating phase of  $\text{Ti}_4\text{O}_7$  also obeys the power-law function  $A(E-E_0)^n$  with  $n \sim 2$ . Moreover, even in the metallic phase, both the spectra of  $\text{CuIr}_2\text{S}_4$  and  $\text{Ti}_4\text{O}_7$  show weak Fermi edges and broad peaks at  $\sim 0.75$  eV, around which most of spectral weights are distributed. Such broad feature is commonly interpreted as the incoherent part of the spectral function accompanying the quasiparticle excitations around  $E_F$ . Probably, the fluctuation of the dimerization may survive at high-temperature metallic phase.

The temperature dependence of the UPS spectra across the MIT is briefly summarized as follows. The  $\text{Ir}^{3+}-\text{Ir}^{3+}-\text{Ir}^{4+}-\text{Ir}^{4+}$  charge ordering and  $\text{Ir}^{4+}-\text{Ir}^{4+}$  dimerization along the (110) or (-110) chains cause the hardgap opening of  $\sim 0.09$  eV, which also manifests in previous studies.<sup>27,31,33,35</sup> On the other hand, the peculiar in-gap state, which shows the power-law behavior with exponent  $n \sim 1.3-1.7$ , gives the anomalous hopping conductivity at low temperature.

## B. Photoexcitation effects

We have also studied photoexcitation effects on the near- $E_F$  UPS spectra. No spectral weight increase at  $E_F$  was observed for any sample surfaces by visible-light irradiation from the Nd:YAG laser up to 5 mJ/pulse ( $8.5 \times 10^{16}$  cm<sup>2</sup> photons/pulse) (see Fig. 5), indicating that the  $\text{Ir}^{3+}/\text{Ir}^{4+}$  charge-ordered gap in the insulating phase is very robust against photoexcitation across the band gap. On the

other hand, the present visible-light irradiation also gives the reduction in the resistance similar to those reported in the x-ray irradiation measurements [Fig. 5(i)]. The weak irradiation up to 1 mJ/pulse ( $1.7 \times 10^{16}$  cm<sup>2</sup> photons/pulse) gives no spectral change near  $E_F$  [Figs. 5(a)–5(e)]. On the other hand, the hump of the in-gap states was decreased by rather strong irradiations of  $\sim 3$ –5 mJ/pulse [Figs. 5(f)–5(h)]. The adsorbates on the surface can be removed by the strong irradiation, and the adsorption rate becomes small after the illumination.

It has been suggested that the long-range charge ordering is destroyed by the x ray.<sup>25,26</sup> Probably, the visible-light irradiation destroys only the phase of  $\text{Ir}^{3+}\text{-Ir}^{3+}\text{-Ir}^{4+}\text{-Ir}^{4+}$  chains in the  $xy$  plane of spinel. When the  $\text{Ir}^{4+}\text{-Ir}^{4+}$  dimers in the  $xy$  chains are shifted to the neighboring sites by the irradiation, the octamer ordering is destroyed (see Fig. 6). This corresponds to the bipolaronic hopping as discussed in Fig. 4 and can be regarded as a kind of bipolaronic solid-to-liquid transition similar to  $\text{Ti}_4\text{O}_7$ .<sup>42</sup> This picture is consistent with the recent diffraction study of  $\text{CuIr}_2\text{S}_4$  at low temperature,<sup>30</sup> indicating that the long-range order (octamer order) is destroyed but the dimers are preserved locally after x-ray or electron irradiation. Moreover similar charge ordering as shown in Fig. 6(b) including  $\text{-Rh}^{3+}\text{-Rh}^{3+}\text{-Rh}^{4+}\text{-Rh}^{4+}$  chains is

observed in the structural study of  $\text{LiRh}_2\text{O}_4$ , which also has Rh sites at the  $B$  site of spinel and shows a metal-insulator transition with some lattice distortion.<sup>43</sup>

#### IV. SUMMARY

We have studied the electronic structure of  $\text{CuIr}_2\text{S}_4$  single crystals using UPS. The UPS data show the band-gap opening of  $\sim 0.09$  eV and support the previous report of  $\text{Ir}^{3+}/\text{Ir}^{4+}$  charge ordering in the insulating phase. The observed in-gap state at low temperature is consistent with the variable range hopping transport. The UPS measurements under laser irradiation indicate that the  $\text{Ir}^{3+}/\text{Ir}^{4+}$  charge disproportionation by the dimer formation is very robust against the photoexcitation but the long-range charge ordering would be destroyed.

#### ACKNOWLEDGMENTS

This work was supported by a Grant-In-Aid for Scientific Research from the Ministry of Education, Culture, Sports, Science, and Technology of Japan (Grant No. 19340092). K.T. acknowledges support from the Japan Society for the Promotion of Science for Young Scientists.

- <sup>1</sup>S. Nakatsuji, V. Dobrosavljević, D. Tanasković, M. Minakata, H. Fukazawa, and Y. Maeno, *Phys. Rev. Lett.* **93**, 146401 (2004).
- <sup>2</sup>A. Husmann, D. S. Jin, Y. V. Zastavker, T. F. Rosenbaum, X. Yao, and J. M. Honig, *Science* **274**, 1874 (1996).
- <sup>3</sup>J. M. D. Coey, M. Viret, L. Ranno, and K. Ounadjela, *Phys. Rev. Lett.* **75**, 3910 (1995).
- <sup>4</sup>T. Yoshida, X. J. Zhou, T. Sasagawa, W. L. Yang, P. V. Bogdanov, A. Lanzara, Z. Hussain, T. Mizokawa, A. Fujimori, H. Eisaki, Z.-X. Shen, T. Kakeshita, and S. Uchida, *Phys. Rev. Lett.* **91**, 027001 (2003).
- <sup>5</sup>S. H. Pan, J. P. O'Neal, R. L. Badzey, C. Chamon, H. Ding, J. R. Engelbrecht, Z. Wang, H. Eisaki, S. Uchida, A. K. Gupta, K.-W. Ng, E. W. Hudson, K. M. Lang, and J. C. Davis, *Nature (London)* **413**, 282 (2001).
- <sup>6</sup>D. D. Sarma, A. Chainani, S. R. Krishnakumar, E. Vescovo, C. Carbone, W. Eberhardt, O. Rader, Ch. Jung, Ch. Hellwig, W. Gudat, H. Srikanth, and A. K. Raychaudhuri, *Phys. Rev. Lett.* **80**, 4004 (1998).
- <sup>7</sup>E. Dagotto, *Nanoscale Phase Separation and Colossal Magnetoresistance* (Springer, Berlin, 2002), and references therein.
- <sup>8</sup>N. Takubo, Y. Ogimoto, M. Nakamura, H. Tamaru, M. Izumi, and K. Miyano, *Phys. Rev. Lett.* **95**, 017404 (2005).
- <sup>9</sup>S. A. Kivelson, I. P. Bindloss, E. Fradkin, V. Oganessian, J. M. Tranquada, A. Kapitulnik, and C. Howald, *Rev. Mod. Phys.* **75**, 1201 (2003).
- <sup>10</sup>S. Nagata, T. Hagino, Y. Seki, and T. Bitoh, *Physica B* **194-196**, 1077 (1994).
- <sup>11</sup>T. Furubayashi, T. Matsumoto, T. Hagino, and S. Nagata, *J. Phys. Soc. Jpn.* **63**, 3333 (1994).
- <sup>12</sup>S. Tsuji, K. Kumagai, N. Matsumoto, and S. Nagata, *Physica C* **282-287**, 1107 (1997).
- <sup>13</sup>M. Hayashi, M. Nakayama, T. Nanba, T. Matsumoto, J. Tang, and S. Nagata, *Physica B* **281-282**, 631 (2000).
- <sup>14</sup>M. Yamamoto, S. Noguchi, H. Ishibashi, and T. Ishida, *Physica B* **329-333**, 940 (2003).
- <sup>15</sup>M. Sasaki, K. Kumagai, K. Kakuyanagi, and S. Nagata, *Physica C* **408-410**, 822 (2004).
- <sup>16</sup>N. L. Wang, G. H. Cao, P. Zheng, G. Li, Z. Fang, T. Xiang, H. Kitazawa, and T. Matsumoto, *Phys. Rev. B* **69**, 153104 (2004).
- <sup>17</sup>A. T. Burkov, T. Nakama, M. Hedo, K. Shintani, K. Yagasaki, N. Matsumoto, and S. Nagata, *Phys. Rev. B* **61**, 10049 (2000).
- <sup>18</sup>K. Yagasaki, T. Nakama, M. Hedo, Y. Uwatoko, Y. Shimoji, S. Notsu, K. Uchima, N. Matsumoto, S. Nagata, H. Okada, H. Fujii, H. Yoshida, H. M. Kimura, Y. Yamaguchi, and A. T. Burkov, *J. Phys. Soc. Jpn.* **75**, 074706 (2006).
- <sup>19</sup>G. Cao, H. Kitazawa, T. Matsumoto, and C. Feng, *Phys. Rev. B* **69**, 045106 (2004); G. Cao, T. Furubayashi, H. Suzuki, H. Kitazawa, T. Matsumoto, and Y. Uwatoko, *ibid.* **64**, 214514 (2001).
- <sup>20</sup>H. Kang, K. Barner, I. V. Medvedeva, P. Mandal, A. Poddar, and E. Gmelin, *J. Alloys Compd.* **267**, 1 (1998).
- <sup>21</sup>N. F. Mott, *Metal-Insulator Transitions*, 2nd ed. (Taylor & Francis, London, 1990).
- <sup>22</sup>A. L. Efros and B. Shklovskii, *J. Phys. C* **8**, L49 (1975).
- <sup>23</sup>P. G. Radaelli, Y. Horibe, M. J. Gutmann, H. Ishibashi, C. H. Chen, R. M. Ibberson, Y. Koyama, Y.-S. Hor, V. Kiryukhin, and S.-W. Cheong, *Nature (London)* **416**, 155 (2002).
- <sup>24</sup>D. I. Khomskii and T. Mizokawa, *Phys. Rev. Lett.* **94**, 156402 (2005).
- <sup>25</sup>H. Ishibashi, T. Y. Koo, Y. S. Hor, A. Borissov, P. G. Radaelli, S. W. Cheong, and V. Kiryukhin, *Phys. Rev. B* **66**, 144424 (2002).
- <sup>26</sup>T. Furubayashi, H. Suzuki, T. Matsumoto, and S. Nagata, *Solid State Commun.* **126**, 617 (2003).

- <sup>27</sup>K. Takubo, S. Hirata, J.-Y. Son, J. W. Quilty, T. Mizokawa, N. Matsumoto, and S. Nagata, *Phys. Rev. Lett.* **95**, 246401 (2005).
- <sup>28</sup>A. Tsujimoto, C. Itoh, and H. Ishibashi (unpublished); *Meet. Abstr. Phys. Soc. Jpn.* **62**, 722 (2007).
- <sup>29</sup>W. Sun, T. Kimoto, T. Furubayashi, T. Matsumoto, S. Ikeda, and S. Nagata, *J. Phys. Soc. Jpn.* **70**, 2817 (2001).
- <sup>30</sup>V. Kiryukhin, Y. Horibe, Y. S. Hor, H. J. Noh, S.-W. Cheong, and C.-H. Chen, *Phys. Rev. Lett.* **97**, 225503 (2006).
- <sup>31</sup>J. Matsuno, T. Mizokawa, A. Fujimori, D. A. Zatsepin, V. R. Galakhov, E. Z. Kurmaev, Y. Kato, and S. Nagata, *Phys. Rev. B* **55**, R15979 (1997).
- <sup>32</sup>E. Z. Kurmaev, V. R. Galakhov, D. A. Zatsepin, V. A. Trofimova, S. Stadler, D. L. Ederer, A. Moewes, M. M. Grush, T. A. Callcott, J. Matsuno, A. Fujimori, and S. Nagata, *Solid State Commun.* **108**, 235 (1998).
- <sup>33</sup>M. Croft, W. Caliebe, H. Woo, T. Tyson, D. Sills, Y. S. Hor, S. W. Cheong, V. Kiryukhin, and S. J. Oh, *Phys. Rev. B* **67**, 201102(R) (2003).
- <sup>34</sup>K. Kitamoto, Y. Taguchi, K. Mimura, K. Ichikawa, O. Aita, and H. Ishibashi, *Phys. Rev. B* **68**, 195124 (2003).
- <sup>35</sup>Han-Jin Noh, E.-J. Cho, H.-D. Kim, J.-Y. Kim, C.-H. Min, B.-G. Park, and S.-W. Cheong, *Phys. Rev. B* **76**, 233106 (2007).
- <sup>36</sup>N. Matsumoto and S. Nagata, *J. Cryst. Growth* **210**, 772 (2000).
- <sup>37</sup>T. Oda, M. Shirai, N. Suzuki, and K. Motizuki, *J. Phys.: Condens. Matter* **7**, 4433 (1995).
- <sup>38</sup>K. Betsuyaku, H. Ishibashi, A. Yanase, and N. Hamada, *J. Magn. Magn. Mater.* **272-276**, e295 (2004).
- <sup>39</sup>J. G. Massey and M. Lee, *Phys. Rev. Lett.* **75**, 4266 (1995).
- <sup>40</sup>T. Sudayama, K. Takubo, T. Mizokawa, S. Nakatsuji, and Y. Maeno (unpublished); *Meet. Abstr. Phys. Soc. Jpn.* **62**, 589 (2007).
- <sup>41</sup>K. Maiti, R. S. Singh, V. R. R. Medicherla, S. Rayaprol, and E. V. Sampathkumaran, *Phys. Rev. Lett.* **95**, 016404 (2005); K. Maiti, *Phys. Rev. B* **73**, 115119 (2006).
- <sup>42</sup>K. Kobayashi, T. Susaki, A. Fujimori, T. Tonogai, and H. Takagi, *Europhys. Lett.* **59**, 868 (2002).
- <sup>43</sup>Y. Okamoto, S. Niitaka, M. Uchida, T. Waki, M. Takigawa, Y. Nakatsu, A. Sekiyama, S. Suga, R. Arita, and H. Takagi, *Phys. Rev. Lett.* **101**, 086404 (2008).